THE MAGNETIC FIELD PILE-UP AND DENSITY DEPLETION IN THE MARTIAN MAGNETOSHEATH: A COMPARISON WITH THE PLASMA DEPLETION LAYER UPSTREAM OF THE EARTH'S MAGNETOPAUSE

MARIT ØIEROSET[1], DAVID L. MITCHELL[1], TAI D. PHAN[1], ROBERT P. LIN[1], DANA H. CRIDER[2] and MARIO H. ACUÑA[1]
[1]*Space Sciences Laboratory, University of California, Berkeley, CA 94720, U.S.A.*
[2]*NASA Goddard Space Flight Center, Code 695, Greenbelt, MD 20771, U.S.A.*

(Accepted in final form 14 March 2003)

Abstract. Using magnetometer and electron observations from the Mars Global Surveyor (MGS) and theWind spacecraft we show that the region of magnetic field pile-up and density decrease located between the Martian ionosphere and bow shock exhibit strong similarities with the plasma depletion layer (PDL) observed upstream of the Earth's magnetopause in the absence of magnetic reconnection when the magnetopause is a solid obstacle in the solar wind. A PDL is formed upstream of the terrestrial magnetopause when the magnetic field piles up against the obstacle and particles in the pile-up region are squeezed away from the high magnetic pressure region along the field lines as the flux tubes convect toward the magnetopause. We here discuss the possibility that at least part of the region of magnetic field pile-up and density depletion upstream of Mars may be formed by the same physical processes which generate the PDL upstream of the Earth's magnetopause. More complete ion, electron, and neutral measurements are needed to conclusively determine the relative importance of the plasma depletion process versus exospheric processes.

Abbreviations: MGS – Mars global surveyor; MPB – magnetic pileup boundary; PDL – plasma depletion layer; PEB – photo electron boundary.

1. Introduction

The nature of the Martian obstacle boundary has been a major topic of debate during the last three decades (e.g., Gringauz *et al.*, 1973; Slavin and Holzer, 1982; Breus *et al.*, 1991; Dubinin *et al.*, 1997; Acuña *et al.*, 1998; Sauer and Dubinin, 2000; Crider *et al.*, 2000). Using observations from the Phobos-2 spacecraft Lundin *et al.* (1991) and Kallio *et al.* (1994) reported that the solar wind plasma flow becomes stagnant several hundred km above the ionosphere, implying the existence of a solar wind obstacle located between the bow shock and the ionosphere, and the possibility that the obstacle was created by an intrinsic magnetic field. However, measurements from MGS revealed that the Martian intrinsic magnetic field consists only of scattered crustal sources and would not be an effective magnetospheric obstacle (Acuña *et al.*, 1998).

The boundary where the proton flow stops was found to be located near, and possibly coincide with the ion composition boundary (ICB) (Breus *et al.*, 1991;

Space Science Reviews **111:** 185–202, 2004.

Sauer *et al.*, 1995). The ICB was defined as a boundary separating solar wind (H^+) dominated plasma from planetary (O^+) dominated plasma (Breus *et al.*, 1991). The ICB was also found to coincide with a boundary termed the planetopause, marked by a disappearance of strong electric field fluctuations (Grard *et al.*, 1989; Trotignon *et al.*, 1996).

Measurements from the MGS spacecraft demonstrated that a permanent feature characterized by strong magnetic field pile-up accompanied by a rather sharp drop in electron fluxes exists upstream of the ionosphere in the vicinity of the Phobos-2 ICB/planetopause (Acuña *et al.*, 1998; Vignes *et al.*, 2000). This feature was termed the magnetic pileup boundary (MPB), after a similar feature observed at comets (Neubauer *et al.*, 1986; Mazelle *et al.*, 1989). The altitude of the MPB has been found to be located closer to the planet when the solar wind pressure is high (Crider et al., 2003). Also, Crider *et al.* (2002) have shown that the altitude where the magnetic field is piling up is higher in the southern hemisphere where the crustal magnetic fields are stronger (Acuña *et al.*, 1999).

Crider *et al.* (2000) interpreted the sharp drop in electron phase space density in this region to be a consequence of electron impact ionization of atmospheric neutrals since the steepest decrease was observed in the 40–150 eV energy range, which is where the cross sections for neutral hydrogen and oxygen are high (Shah *et al.*, 1987; Thompson *et al.*, 1995). In the proposed electron impact ionization process incident electrons lose kinetic energy when they impact an exospheric particle and a secondary electron with lower energy is produced.

The magnetic field pile-up in the region of electron depletion has recently been attributed to charge exchange between solar wind protons and atmospheric neutrals (Chen *et al.*, 2001). In the Chen *et al.* model a magnetic field increase in good agreement with that observed by MGS is produced by assuming that ion pressure lost by charge exchange is compensated for by an increase in magnetic pressure.

At Earth a similar increase in magnetic field magnitude and an associated decrease in electron fluxes have been observed immediately upstream of the Earth's magnetopause, where it has been linked to the existence of a plasma depletion layer (PDL) (e.g., Paschmann *et al.*, 1978; Crooker *et al.*, 1979; Fuselier *et al.*, 1991; Song *et al.*, 1993; Anderson and Fuselier, 1993; Anderson *et al.*, 1994; Phan *et al.*, 1994). A PDL is formed by the pile-up of magnetosheath field lines against the magnetopause in the absence of magnetopause reconnection, when the magnetopause becomes a solid obstacle in the solar wind, and is favored for northward interplanetary magnetic field (when the magnetosheath and the dayside magnetospheric fields are parallel) and high solar wind pressure (Anderson *et al.*, 1997). Particles in the field pile-up region are squeezed away from the high magnetic pressure region along the field lines as the flux tubes convect toward the magnetopause, leading to a decrease first in the higher energy fluxes, later in the lower energies (Zwan and Wolf, 1976; Paschmann *et al.*, 1993). Increasing ion temperature anisotropy ($T_\perp \gg T_\parallel$) and enhanced magnetosheath flow perpendicular to the magnetic field are observed in the PDL (Phan *et al.*, 1994). The enhancement

of the perpendicular flow results from acceleration by magnetic tension associated with field lines being draped around the solid obstacle (Phan *et al.*, 1994). Mirror mode waves, common in the high beta magnetosheath, tend to be damped in the low beta PDL where the mirror condition $T_\perp/T_\parallel - (1 + /\beta_\perp) \geq 0$ is no longer satisfied (Anderson and Fuselier, 1993; Phan *et al.*, 1994). Zwan and Wolf (1976) postulated that a PDL should form in front of any planetary boundary, for example upstream of Venus and Mars, if the obstacle is effectively impenetrable. The PDL process is not related to impact ionization.

In this paper we compare the magnetic field pile-up and density depletion observed upstream of Mars by MGS with observations of the terrestrial PDL made by the Wind spacecraft. We show that the two regions have quite similar particle and field characteristics and raise the possibility that at least part of the region of magnetic field pile-up observed upstream of Mars may be a PDL. More complete ion and electron measurements are needed to conclusively determine the relative importance of plasma depletion versus exospheric processes.

2. Instrumentation

Observations from the Martian plasma environment are obtained by the Mars Global Surveyor (MGS) spacecraft. The magnetometer/electron reflectometer (MAG/ER) experiment onboard the MGS spacecraft is described in Acuña *et al.* (1998). In the present study a magnetic field resolution of 0.3 s has been used. The electron distribution function is measured in the range from $\sim$ 10 eV to 20 keV every 2 to 12 s, depending on the energy channel. The ER does not provide full 3D measurements, but the electron density above $\sim$ 10 eV can be reliably estimated. The electron temperature above the ionosphere have been estimated by fitting the measurements to a Maxwellian distribution, assuming isotropy. The electron bulk flow velocity cannot be reliably estimated from the ER measurements.

The Wind spacecraft provides full 3D plasma and magnetic field measurements from the Earth's magnetosheath. Averaged ion distribution functions are obtained every 51 s from the three-dimensional 'top-hat' electrostatic analyzer, operating in a mode to detect particles with energies from 80 eV to 27 keV. Electron distribution functions are measured every 51 s, covering energies from 10 eV to 27 keV. The magnetic field instrument onboard Wind measures the magnetic field at a rate of 10.9 samples s^{-1}, but for our analysis the magnetic field data are averaged over the 3-s spin period. Details of the Wind plasma and magnetic field instruments are described by Lin *et al.* (1995) and Lepping *et al.* (1995), respectively.

To analyze the region of magnetic field pile-up upstream of the obstacles we use the LMN boundary normal coordinate system (see Figure 1). The N axis points outward away from the planet along the boundary normal and the (L,M) plane is tangential to the boundary with L oriented in the direction of maximum variance of the magnetic field and M along the intermediate variance direction. λ is the angle

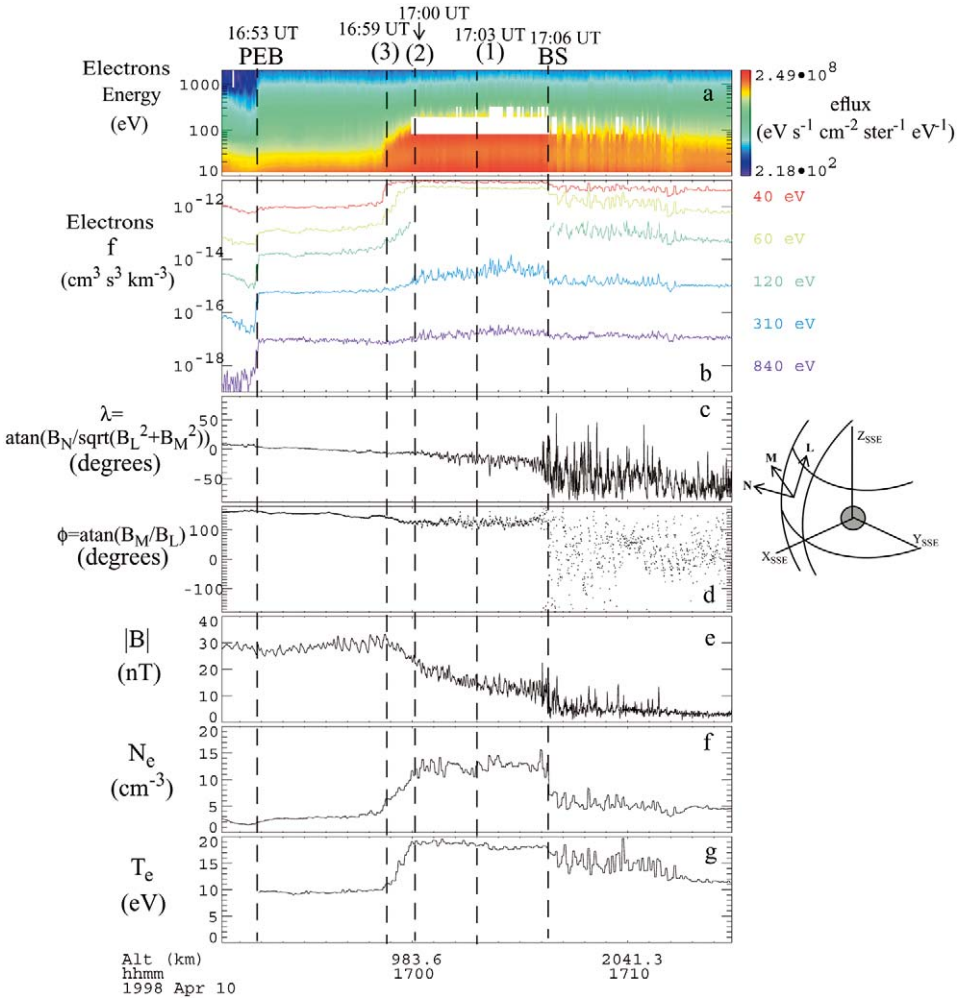

Figure 1. MGS observations from SPO 231 on April 10, 1998. The LMN coordinate system defined in the text is shown to the right in the figure. (a) Electron energy spectrogram. Some data points are missing due to instrument saturation; (b) electron phase space density for the 40–840 eV energy bins; (c) the λ magnetic field angle (angle between **B** and the (*L,M*) plane); (d) the ϕ magnetic field angle (angle of **B** in the (*L,M*) plane); (e) the magnitude of the magnetic field; (f) the electron density; (g) the electron temperature. The bow shock and the photoelectron boundary are marked with the vertical dashed lines 'BS' and 'PEB'. The vertical lines (1), (2), and (3) are explained in the text.

between **B** and the (*L,M*) plane while ϕ is the angle of **B** in the (*L,M*) plane, with 0° along L. The boundary normal direction was found using minimum variance analysis of the magnetic field (Sonnerup and Cahill, 1967).

3. MGS Observations

We here present two typical examples of magnetic field pile-up and density depletion in the prenoon sector upstream of Mars. Both examples are from the elliptical science phasing orbits (SPO) where the Martian magnetosheath was sampled at high latitudes. The first example has been discussed previously by Crider *et al.* (2000).

3.1. First MGS example

Figure 1 shows data from SPO 231 on April 10, 1998, when MGS was in a polar elliptical 10 LT orbit with perigee near the north pole. Going back in time from right to left in the plot, MGS encountered the bow shock at 17:06 UT (marked by the dashed line 'BS') and entered the turbulent (Figure 1(e)), high density (Figure 1(f)) magnetosheath. Until $\sim$17:03 UT (marked by the dashed line '(1)' in Figure 1) the magnetosheath magnetic field stayed rather constant at a $\sim$13 nT magnitude with $\sim$5 nT amplitude fluctuations (Figure 1(e)). These magnetic field fluctuations are anti-correlated with the density fluctuations and hence likely to be mirror mode waves, common in high beta plasmas (Tsurutani *et al.*, 1982). The amplitude of the waves diminishes when the magnetic field piles up (Figure 1(e)). From 17:03 UT to 16:59 UT (marked by '(3)' in Figure 1) a steady increase in magnetic field magnitude from 13 nT to 30 nT was observed. After 16:59 UT the magnetic field magnitude stayed rather constant. The spacecraft encountered the photoelectron boundary (PEB) in the vicinity of the ionopause (Mitchell *et al.*, 2000) at 16:53 UT, marked by the sharp drop in high energy (120–840 eV) electron phase space density (Figure 1(b)). The angle λ (Figure 1(c)) was close to zero during the interval of magnetic field pile-up (between (1) and PEB), implying that the normal component of the magnetic field stayed rather constant and small. The gradual rotation in λ from $\sim$ 10° at (1) to $\sim$ 0° at the PEB indicates that the magnetic field became increasingly more draped. A slow gradual rotation in ϕ (Figure 1(d)) was also seen.

The electron density (Figure 1(f)) dropped from $\sim$ 13 cm^{-3} at (1) to $\sim$8 cm^{-3} at (3) while the electron temperature (Figure 1(g)) decreased from $\sim$19 eV to $\sim$11 eV. The density and temperature stayed rather constant between (3) and the PEB. The variations in flux levels depend strongly on the energy. The high-energy levels (310 eV and 840 eV) started to decrease smoothly already near the bow shock and reached a stable level after 16:59 UT (3). The 60 eV channel, on the other hand, showed only little variation until 17:00 UT when the flux levels dropped rather sharply (marked by '(2)' in Figure 1) and continued to drop until the spacecraft reached the PEB. There is a data gap in the 120 eV channel between 17:06 UT and 17:00 UT due to saturation, but this channel also dropped sharply from (2) to (3). The 40 eV channel started to decrease even later, at $\sim$16:59 UT. The region between (2) and (3) was termed the magnetic pile-up boundary (MPB)

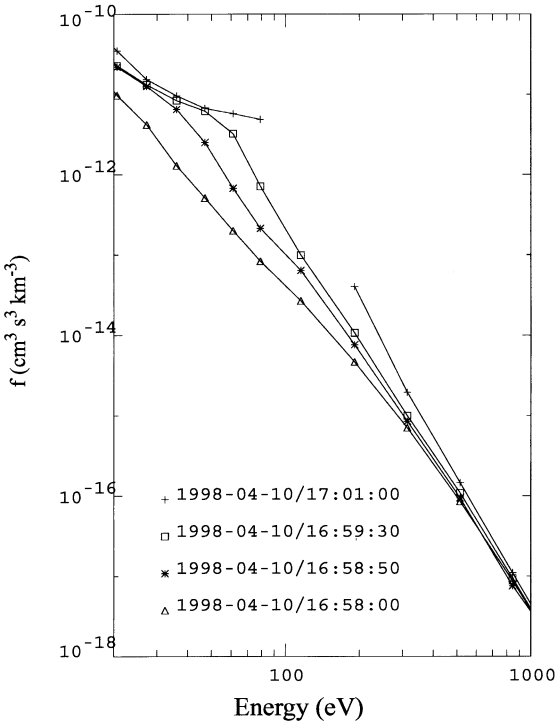

Figure 2. Development of electron spectra in the region where the magnetic field piles up observed by MGS on SPO 231 on April 10, 1998. After Crider *et al.* (2000).

and the steep drop in the 40–120 eV phase space density between (2) and (3) was interpreted to be a signature of electron impact ionization by Crider *et al.* (2000). Mazelle *et al.* (2002) also suggested that the term 'MPB' be used for the relatively steep increase in magnetic field magnitude seen between (2) and (3), analogous to what is observed at comets (Mazelle *et al.*, 1989), while they called the region planetward of (3) the magnetic pile-up region.

The development of the electron distribution function through the region where the magnetic field is piling up is shown in Figure 2. This figure is similar to Figure 2 in Crider *et al.* (2000). At 17:01:00 UT, right before the density depletion started, the spectrum was a typical post-shock magnetosheath spectrum. At 16:58:00 UT, when the magnetic field had stopped increasing, electrons with energies between $\sim$20 eV and $\sim$200 eV had been significantly depleted (almost two orders of magnitude at $\sim$80 eV).

3.2. SECOND MGS EXAMPLE

Figure 3 shows data from SPO 233 on April 11, 1998, when MGS was still in its polar elliptical 10 LT orbit with perigee near the north pole. Again going backwards in time, MGS encountered the bow shock at 16:29 UT (marked by the dashed line

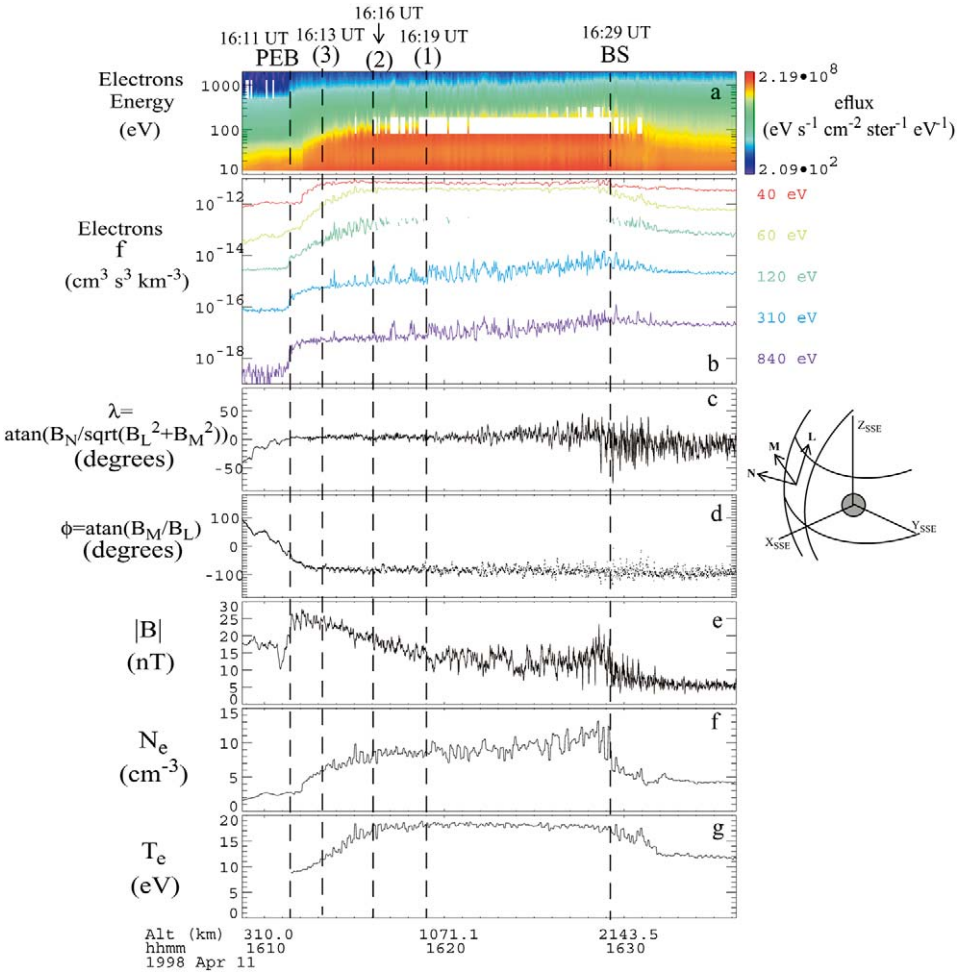

Figure 3. MGS observations from SPO 233 on April 11, 1998. The panels are explained in the caption of Figure 1. The LMN coordinate system defined in the text is shown to the right in the figure.

'BS') and entered the magnetosheath. Until ∼16:19 UT (1) the magnetosheath magnetic field magnitude (Figure 2e) stayed rather constant at ∼12 nT. Magnetic field fluctuations anti-correlated with density fluctuations were again observed and the wave amplitude diminished as the magnetic field piled up (Figure 2(e)). As mentioned before these waves are likely to be mirror mode waves. From 16:19 UT (1) to 16:13 UT (3) a steady increase in magnetic field magnitude from 12 nT to 24 nT was observed. After 16:13 UT the magnetic field magnitude stayed rather constant until the spacecraft encountered the PEB in the vicinity of the ionosphere at 16:11 UT, marked by the sharp drop in the 120–840 eV electron phase space density (Figure 2(b)). The angle λ (Figure 2(c)) was small and approaching zero during the interval of magnetic field pile-up (between (3) and PEB), implying that

the normal component of the magnetic field stayed rather constant and small and that the draping of the magnetic field became increasingly stronger (see also Bertucci *et al.*, 2002). In contrast to the first example (Figure 1) a gradual rotation of $\sim 40^\circ$ was seen in the ϕ angle (Figure 2(d)) from 16:13 UT to 16:11 UT when the spacecraft entered the PEB. The rotation started at (3), at the time when the magnetic field stopped increasing.

The electron density (Figure 2(f)) dropped from ~ 9 cm^{-3} at (1) to ~ 7 cm^{-3} at (3) while the electron temperature (Figure 2(g)) decreased from ~ 18 eV to ~ 11 eV. The density and temperature continued to decrease until the PEB. As in the previous example (Figure 1) the variations in flux levels depend strongly on the energy (Figure 2b). The high energy levels (310 eV and 840 eV) started to decrease smoothly near the bow shock and continued to decrease until the PEB. The 120 eV and 60 eV channels, on the other hand, showed only little variation until 16:16 UT (marked by '(2)' in Figure 1) when the flux levels dropped rather sharply and continued to drop until the spacecraft reached the PEB. The 40 eV channel started to decrease even later, at 16:14 UT.

3.3. Key features of the region of magnetic field pile-up upstream of Mars

As shown in the two examples presented above the following features are typically present in the region between the bow shock and the ionosphere at Mars:

(1) The magnetic field piles up and when the piling up has reached a certain point the electron density and temperature decreases.

(2) The electron phase space density drops earlier at higher energies than at lower energies.

(3) The magnetic field becomes increasingly more draped around the Martian obstacle as the magnetic field piles up.

(4) The magnetic field lines are nearly perfectly draped in the region planetward of where the maximum magnetic field magnitude is observed.

(5) In the second example (Figure 3) a rotation in the ϕ angle coincides with where the magnetic field stops increasing. This could imply a current sheet at this location.

4. Wind Observations

For comparison with the MGS observations we here review two examples of plasma depletion layer (PDL) observed upstream of the Earth's magnetopause. The first example is from aWind flank crossing, ideal for comparison with the MGS flank crossings presented above. The second example is from a Wind subsolar crossing.

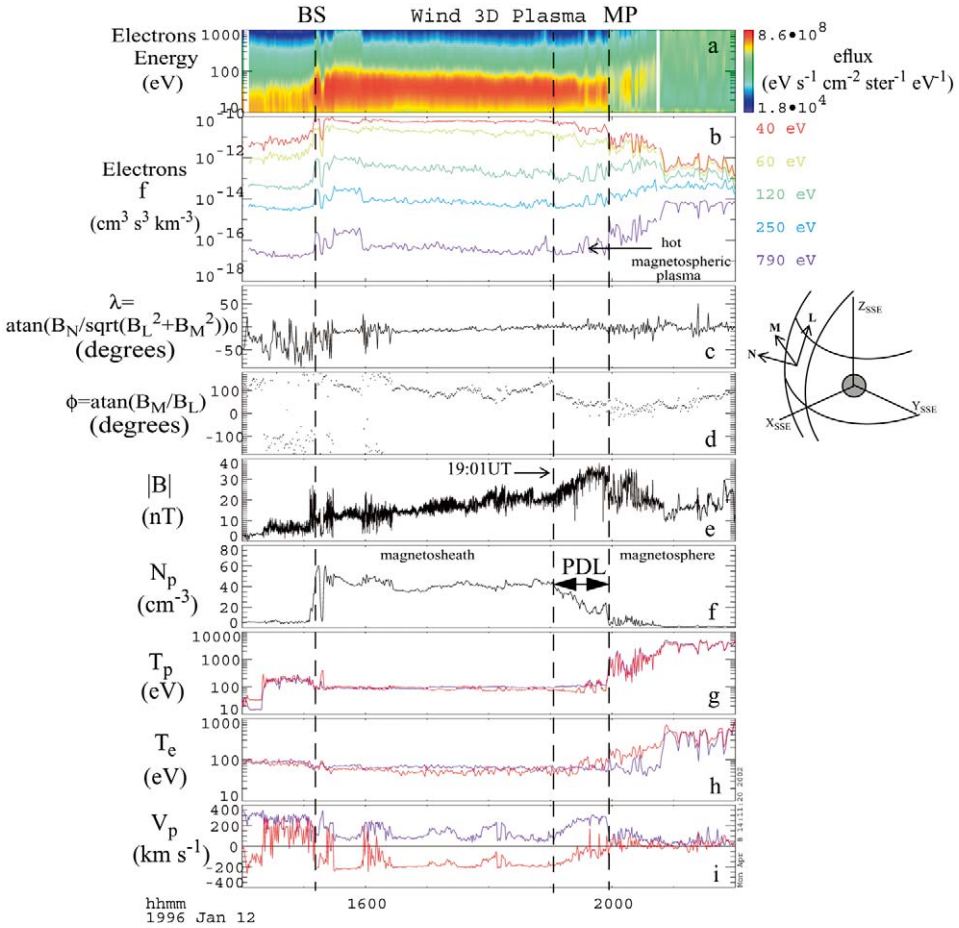

Figure 4. Wind observations from January 12, 1996. (a) Electron energy spectrogram; (b) Electron phase space density for the 40–790 eV bins; (c) the λ magnetic field angle; (d) the ϕ magnetic field angle; (e) the magnitude of the magnetic field; (f) the proton density; (g) the parallel (red) and perpendicular (blue) proton temperature; (h) the parallel (red) and perpendicular (blue) electron temperature; (i) proton velocity shown as the component perpendicular (blue) and parallel (red) to the magnetic field. The bow shock (BS), magnetopause (MP), and the onset of the PDL are marked with vertical dashed lines. Multiple crossings of the bow shock took place on this day and the bow shock (BS) is marked at the time of the first bow shock crossing. The LMN coordinate system defined in the text is shown to the right in the figure.

4.1. First Wind Example: Flank PDL

On January 12, 1996, Wind crossed the low shear dusk flank magnetopause near 18 LT. The event was analyzed in detail by Phan *et al.* (1997) and in Figure 4 we present an overview of the measurements relevant for the MGS comparison. The spacecraft encountered the bowshock at 15:08 UT and spent almost 5 hours in the magnetosheath before it crossed the magnetopause at 19:55 UT. The PDL

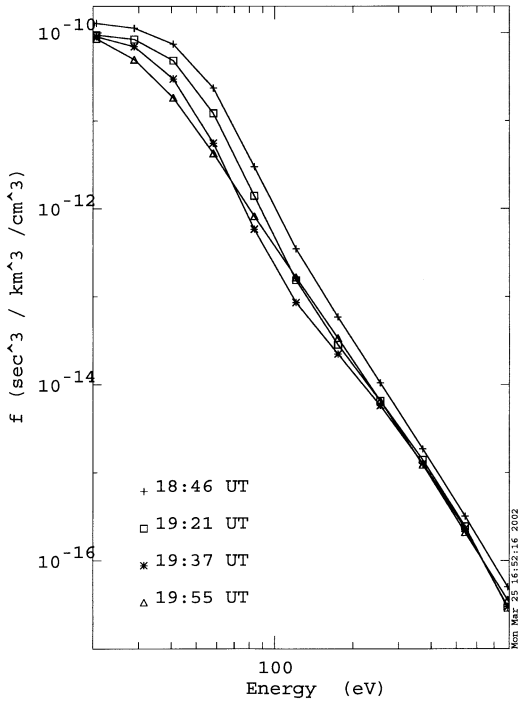

Figure 5. Development of the electron spectra observed by Wind in the PDL on January 12, 1996.

was observed from ∼19:01 UT when the proton density (Figure 4(f)) started to drop and the magnetic field magnitude (Figure 4(e)) started to increase strongly (Phan *et al.*, 1997). The density had dropped more than 60%, from ∼44 cm^{-3} in the pre-pile-up magnetosheath to ∼15 cm^{-3} when the spacecraft encountered the magnetopause, and the simultaneous magnetic field increase was ∼30% (from ∼20 nT to ∼33 nT). The λ angle (Figure 4(c)) gradually moved towards zero as the spacecraft approached the magnetopause, implying that the magnetic field lines became more and more draped around the magnetopause. The ϕ angle (Figure 4(d)) exhibited a rather abrupt rotation at the start of the PDL associated with a rotation of the interplanetary magnetic field while no significant rotation was seen across the magnetopause, indicating a low magnetic shear magnetopause. In the PDL the parallel proton temperature (red line) dropped while the perpendicular temperature (blue line) remained constant (Figure 4(g)). No significant anisotropy was observed in the electron temperature (Figure 4(h)). The perpendicular proton velocity increased in the PDL while the parallel velocity decreased to ∼zero (Figure 4(i)). Mirror mode waves were observed throughout the magnetosheath and the PDL (Figure 4(e)). Mirror mode waves were identified based on the fact that the mirror condition ($T_\perp/T_\parallel - (1 + 1/\beta_\perp) \geq 0$) was marginally satisfied (Phan *et al.*, 1997).

The decrease in flux levels was different for the low and high-energy channels (Figure 4(b)). The 250 eV and 790 eV flux levels started to drop right after the

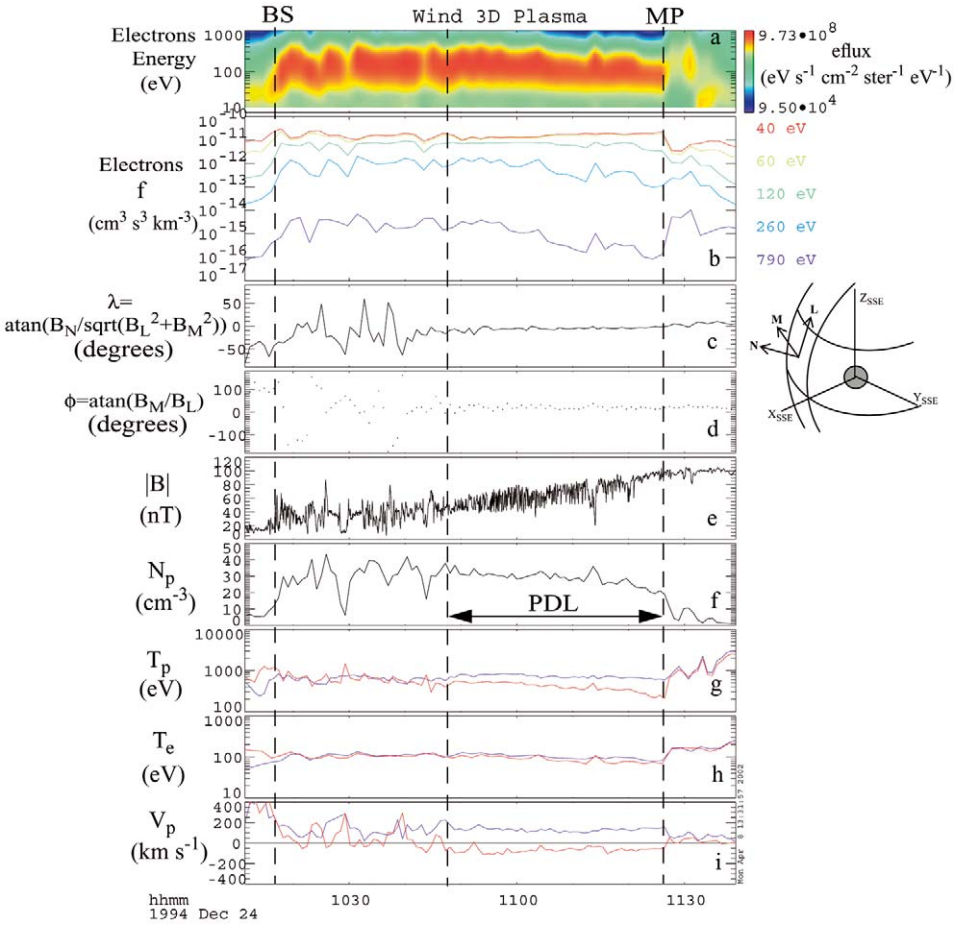

Figure 6. Wind observations from December 24, 1994. The panels are explained in the caption of Figure 4.

bow shock and the flux levels had reached a rather constant level inside the PDL. The 60 eV and 120 eV channels also decreased smoothly from the bow shock but exhibited a steeper drop inside the PDL. The 40 eV flux level stayed rather constant throughout the magnetosheath, started to decrease inside the PDL, and finally dropped sharply at 19:26 UT, approximately midway through the PDL. Hot plasma leaking from the magnetosphere (marked in Figure 4) was seen in the PDL as the spacecraft moved closer to the magnetopause.

The development of the electron distribution function as Wind moved through the PDL is shown in Figure 5. At 18:46 UT, before the density depletion started, the spectrum was a typical terrestrial post-shock magnetosheath spectrum. The shape of the post-shock spectrum at Mars (Figure 2) and Earth are somewhat different, with an enhancement in the 50–200 eV phase space density at Mars compared to the Earth. At Mars the drop in the 50–200 eV electron phase space density

across the region of strong magnetic field pile-up was between one and two orders of magnitude (Figure 2), while the terrestrial magnetosheath spectrum drops more evenly. At 19:55 UT (Figure 5), just before encountering the magnetopause, electrons with energies between ~ 20 eV and ~ 200 eV had been significantly depleted (almost an order of magnitude between 30 eV and 100 eV). The distribution function declined first at higher energies, then later at lower energies, similar to what is observed in this region upstream of Mars (Figure 2). For the last spectrum, obtained at 19:55 UT near the magnetopause, the effect of leakage of hot magnetospheric plasma is evident in the higher energies.

4.2. SECOND WIND EXAMPLE: SUBSOLAR PDL

The data shown in Figure 6 are from December 24, 1994, whenWind crossed the subsolar terrestrial magnetosheath in the ecliptic plane. This event was presented in detail by Phan *et al.* (1996) and we here summarize some aspects of the event.

The Wind spacecraft encountered the bow shock at 10:16 UT and spent 70 min in the magnetosheath before it crossed the Earth's magnetopause at 11:26 UT. From approximately 10:49 UT a gradual decrease in the magnetosheath plasma density was seen (Figure 6(f)), marking the beginning of the PDL. This decrease in density continued until the spacecraft encountered the magnetopause where the density had dropped by 30% from ~ 30 cm^{-3} to ~ 20 cm^{-3}. During the interval of density decrease strong piling up of the magnetic field was observed (Figure 6(e)). The magnetic field magnitude increased from 45 nT at 10:49 UT to 97 nT at the magnetopause 37 min later. The λ angle (Figure 6(c)) gradually moved towards zero as the spacecraft approached the magnetopause, implying that the magnetic field lines became more and more draped around the magnetopause. The ϕ angle (Figure 6(d)) stayed close to zero throughout the PDL. No significant rotation was seen across the magnetopause, consistent with a low magnetic shear (no reconnection) magnetopause. The ion and electron temperature (Figure 6(g) and 6h) exhibited strong anisotropies in the interval of density decrease/magnetic field pile-up. The parallel proton velocity decreased inside the PDL while the perpendicular velocity stayed rather constant (Figure 6(i)).

Mirror mode waves were seen throughout the magnetosheath and the fluctuation amplitude decreased as Wind entered deeper into the PDL (Phan *et al.*, 1996). The damping of the mirror mode waves took place when the mirror condition $(T_\perp/T_\parallel - (1 + 1/\beta_\perp) \geq 0)$ was no longer satisfied in this low beta region (Phan *et al.*, 1996).

The decrease in flux levels was again different for the low and high energy channels (Figure 6(b)). The 250 eV and 790 eV flux levels started to decrease earlier than the 120 eV channel. In this case the 40 eV and 60 eV phase space density stayed approximately constant throughout the PDL.

4.3. KEY FEATURES OF THE PDL

The flank example and the subsolar example presented above are qualitatively similar. Based on the two examples we find the following features to be characteristic for the PDL upstream of the Earth's magnetopause when magnetic reconnection is not operating:

(1) Magnetic field increase

(2) Density decrease

(3) Enhanced ion temperature perpendicular to the magnetic field

(4) Enhanced flow perpendicular to the magnetic field

(5) Electron phase space density drops earlier at higher energies than at lower energies

(6) Magnetic field becomes increasingly more draped around the magnetopause as the magnetic field piles up

(7) Mirror mode waves, observed throughout the magnetosheath, are damped in the PDL when the mirror condition is no longer satisfied.

5. Discussion

5.1. COMPARISON BETWEEN THE MAGNETIC FIELD PILE-UP AND DENSITY DECREASE OBSERVED UPSTREAM OF MARS AND EARTH

The examples above show that the magnetic field and electron properties in the region where the magnetic field is piling up upstream of Mars strongly resemble those observed in the PDL upstream of the Earth's magnetopause. At Mars the electron density dropped 40% (Figure 1) and 20% (Figure 3) from the post-shock magnetosheath to the end of the magnetic field pile-up, while the corresponding density decrease upstream of the Earth was 60% for the flank example (Figure 4) and 30% for the subsolar PDL example (Figure 6). The magnetic field increase upstream of both Mars and Earth was a factor of ~ 2. Mirror waves were observed in both the terrestrial and the Martian magnetosheath. These waves tend to be damped in the subsolar terrestrial PDL (Anderson and Fuselier, 1993; Phan *et al.*, 1994). However, mirror waves may persist in the flank PDL where the magnetic field magnitude is small and the mirror condition still satisfied (e.g., Figure 4). As shown in Figures 1 and 3 the mirror mode waves are damped but still present in the region of strong magnetic field pile-up upstream of Mars, consistent with observations from the flank PDL at Earth (Figure 4). For both Mars and Earth the magnetic field becomes increasingly more draped in the region where the magnetic field is piling up.

The behavior of the electron phase space density levels in front of the two obstacles (Mars and Earth) is remarkably similar, with a gradual decrease in the higher energy channels starting already near the bow shock with the lower energy channels dropping only later, inside the region where the magnetic field increases

(Figures 1–3). In other words, upstream of both planets the distribution function first declines at the highest energy ($\sim$1 keV) and the decrease in phase space density becomes stronger as the energy gets lower (Figures 2 and 5). At the lowest energy ($\sim$20 eV), however, the decrease is not as strong. At Mars the largest drop in phase space density is seen in the 50–150 eV energy bins with a decrease of almost two orders of magnitude for the 80 eV bin. In the Earth's PDL one order of magnitude decrease in electron phase space density is seen for the 40–80 eV bins.

The slow decrease in the higher energy phase space density from the bow shock throughout the magnetosheath can be explained in terms of a gas-dynamic effect (Spreiter *et al.*, 1966), while the sharper drop in phase space density for the lower ($<$ 120 eV) energy bins is not predicted by gas-dynamics.

Crider *et al.* (2000) interpreted the sharp drop in the 40–150 eV electron phase space density observed in the region where the magnetic field is piling up between the Martian ionosphere and bow shock to be a consequence of electron impact ionization of atmospheric neutrals since the 40–150 eV energy range is where the cross sections for neutral hydrogen and oxygen are high (Shah *et al.*, 1987; Thompson *et al.*, 1995). The increase in low energies that should result from the secondary electrons was not observed, although it is possible that most of the secondary electrons may fall below the detection limit of the ER instrument onboard MGS. The fact that the low-energy secondary electrons were not observed could be interpreted as evidence for the plasma depletion process being important at Mars since plasma depletion could account for some of the observed density decrease.

Although electron impact ionization may be important in the solar wind interaction with Mars (Crider *et al.*, 2000) and comets (Cravens *et al.*, 1987) this process cannot explain the rather sharp decrease in the lower energy bins (40–80 eV) observed in the PDL outside the Earth's magnetopause, where the effects of exospheric processes are absent. In the Earth's PDL the density depletion is generated when particles are squeezed away along the field lines from the strong magnetic field region with the higher energy particles disappearing first, followed later by the lower energies (e.g., Song *et al.*, 1993; Paschmann *et al.*, 1993). This depletion does not depend on the process in which the strong magnetic field region was created, i.e., whether the increase is due to a simple compression of the magnetic field against the solar wind obstacle boundary (Zwan and Wolf, 1976), or whether the strong magnetic field has been produced by charge exchange, as suggested by Chen *et al.* (2001).

5.2. Predictions of PDL ion signatures for future Mars missions

We can exclude that exospheric phenomena produce the PDL observed upstream of the Earth's magnetosphere since the Earth lacks an extended exosphere with significant density. However, the question of whether the magnetic field pile-up and density depletion upstream of Mars is an 'Earth-like' PDL or generated by exospheric processes cannot be fully answered using the existing MGS measurements.

Full three-dimensional ion and electron measurements, as well as observations of the neutrals are needed.With threedimensional ion measurements one will be able to determine whether the ion temperature and flow perpendicular to the magnetic field is enhanced in the region of magnetic field pile-up. Such an observation would imply the existence of a PDL upstream of Mars.

A possible scenario would be a magnetic field pile-up and density decrease which is partly caused by plasma depletion and partly caused by exospheric processes. A one order of magnitude decrease in the 80 eV phase space density is observed upstream of the Earth's magnetopause (Figure 5) and hence the plasma depletion process could explain a similar decrease upstream of Mars. However, the corresponding decrease in the 80 eV electron phase space density upstream of Mars is two orders of magnitude, suggesting that additional processes, like e.g. electron impact ionization (Crider *et al.*, 2000), are operative in depleting the electrons (Figure 2). Future missions to Mars carrying full three-dimensional ion and electron instruments will be able to determine the relative contribution from the plasma depletion process and from exospheric phenomena. ESA's Mars Express is equipped to study the possible existence of a PDL upstream of Mars.

5.3. Consequences of a Martian PDL on the location of the Martian obstacle boundary

If a PDL exists upstream of Mars it implies that the Martian solar wind obstacle boundary is located at the inner edge of this PDL, i.e., where the magnetic field reaches its maximum value (Zwan and Wolf, 1976). The observed rotation in the magnetic field at this location (see Figure 3) could indicate the presence of a boundary. Phobos-2 observations suggest that the ion composition boundary (ICB), a boundary separating solar wind (H^+) dominated plasma from planetary (O^+) dominated plasma, is located in the region where the proton flow becomes stagnant (Breus *et al.*, 1991; Kallio *et al.*, 1994; Sauer *et al.*, 1995). Hence the flow of plasma is slowed down by mass loading of atmospheric neutrals and the magnetic field carried by this plasma will become nearly stagnant, giving rise to an (induced) solar wind obstacle with an obstacle boundary located at some altitude above the PEB. The average location of strong magnetic field pile-up upstream of Mars is indeed found to be located near the ICB, several hundred km above the PEB (Vignes *et al.*, 2000).

6. Summary

The piling up of magnetic field and the associated decrease in density upstream of Mars exhibit strong similarities with the plasma depletion layer (PDL) observed upstream of the Earth's magnetopause when reconnection is absent. The plasma depletion process can account for at least one order of magnitude decrease in the

electron phase space density (Figure 5). It is therefore possible that the observed density decrease upstream of Mars is in part caused by this process. Electron impact ionization may account for the observed additional decrease in phase space density. The exact nature of the Martian solar wind obstacle remains unknown.

Acknowledgements

We thank Ron Lepping, the principal investigator of the Wind magnetic field experiment, for making the Wind magnetic field data available. We would like to thank Christian Mazelle, David Sibeck, Laura Peticolas,Yue Chen, Esa Kallio, and Konrad Sauer for helpful discussions. This work benefited greatly from the workshop on Mars magnetism and its interaction with the solar wind, held at the International Space Science Institute (ISSI) in Bern, Switzerland on October 22 –26, 2001, sponsored by ISSI and NASA/JPL/MGS. This research was funded in part by NASA grants NAG5-959, NAG5-6928, and NAG5-10428 at U.C. Berkeley.

References

Acuña, M. H. *et al.*: 1998, 'Field and Plasma Observations at Mars: Initial Results of the Mars Global Surveyor Mission', *Science* **279**, 1676.

Acuña, M. H. *et al.*: 1999, 'Global Distribution of Crustal Magnetization Discovered by the Mars Global Surveyor MAG/ER Experiment', *Science* **184**, 790.

Anderson, B. J. and Fuselier, S. A.: 1993, 'Magnetic Pulsations from 0.1 to 4.0 Hz and Associated Plasma Properties in the Earth's subsolar Magnetosheath and Plasma Depletion Layer', *J. Geophys. Res.* **98**, 1461.

Anderson, B. J., Fuselier, S. A., Gary, S. P. and Denton, R. E.: 1994, 'Magnetic Spectral Signatures in the Earth's Magnetosheath and Plasma Depletion Layer', *J. Geophys. Res.* **98**, 1461.

Anderson, B. J., Phan, T. D. and Fuselier, S. A.: 1997, 'Relationships Between Plasma Depletion and Subsolar Reconnection', *J. Geophys. Res.* **102**, 9531.

Bertucci, C. *et al.*: 2002, 'Magnetic Field Draping Enhancement at the Magnetic Pileup Boundary of Mars from Mars Global Surveyor Observations', submitted to *Geophys. Res. Lett.*

Breus, T. K., Krymskii, A. M., Lundin, R., Dubinin, E. M., Luhmann, J. G., Yeroshenko, Y. G., Barabash, S. V., Mitnitskii, V. Y., Pissarenko, N. F. and Styashkin, V. A.: 1991, 'The Solar Wind Interaction with Mars: Consideration of Phobos 2 Mission Observations of an Ion Composition Boundary on the Dayside', *J. Geophys. Res.* **96**, 11 165.

Chen, Y., Cloutier, P. A., Crider, D. H., Mazelle, C. and Rème, H.: 2001, 'On the Role of Charge Exchange in the Formation of the Martian Magnetic Pile-up Boundary', *J. Geophys. Res.* **106**, 29 387.

Cravens, T. E., Kozyra, J. U., Nagy, A. F., Gombosi, T. I. and Kurtz, M.: 1987, 'Electron Impact Ionization in the Vicinity of Comets', *J. Geophys. Res.* **92**, 7341.

Crider, D. H. *et al.*: 2000, 'Evidence of Electron Impact Ionization in the Magnetic Pileup Boundary of Mars', *Geophys. Res. Lett.* **27**, 45.

Crider, D. H. *et al.*: 2002, 'Observations of the Latitude Dependence of the Location of the Martian Magnetic Pileup Boundary', *Geophys. Res. Lett.* (in press).

Crider, D. H., Vignes, D., Krymskii, A. M., Breus, T. K., Ness, N. F., Mitchell, D. L. et al.: 2003, 'A Proxy for Determining Solar Wind Dynamic Pressure at Mars using Mars Global Surveyor Data; *J. Geophys. Res.* **108** (A12): 1461, 10.1029/2003JA009875.

Crooker, N. U., Eastman, T. E. and Stiles, G. S.: 1979, 'Observations of Plasma Depletion in the Magnetosheath at the Dayside Magnetopause', *J. Geophys. Res.* **84**, 869.

Dubinin, E. M., Sauer, K., Baumgärtel, K. and Lundin, R.: 1997, 'The Martian Magnetosheath: Phobos-2 Observations', *Adv. Space Sci.* **20**, 149.

Fuselier, S. A., Klumpar, D. M., Shelley, E. G., Anderson, B. J. and Coates, A. J.: 1991, 'He(2^+) and H($^+$) Dynamics in the Subsolar Magnetosheath and Plasma Depletion Layer', *J. Geophys. Res.* **96**, 21 095.

Grard, R., Pedersen, A., Klimov, S., Savin, S. and Skalskii, A.: 1989, 'First Measurements of Plasma Waves near Mars', *Nature* **341**, 607.

Gringauz, K. I., Bezrukikh, V. V., Volkov, G. I., Breus, T. K., Musatov, I. S., Havkin, L. P. and Sloutchonkov, G. P.: 1973, 'Preliminary Results on Plasma Electrons from Mars-2 and Mars-3', *Icarus* **18**, 54.

Kallio, E., Koskinen, H., Barabash, S., Lundin, R., Norberg, O. and Luhmann, J. G.: 1994, 'Proton Flow in the Martian Magnetosheath', *J. Geophys. Res.* **99**, 23 547.

Lepping, R. P. *et al.*: 1995, 'The Wind Magnetic Field Investigation', *Space Sci. Rev.* **71**, 207.

Lin, R. P. *et al.*: 1995, 'A Three-Dimensional Plasma and Energetic Particle Investigation for the Wind Spacecraft', *Space Sci. Rev.* **71**, 125.

Lundin, R., Norberg, O., Dubinin, E. M., Pisarenko, N. and Koskinen, H.: 1991, 'On the Momentum Transfer of the Solar Wind to the Martian Topside Ionosphere', *Geophys. Res. Lett.* **18**, 1059.

Mazelle, C. *et al.*: 1989, 'Analysis of Suprathermal Electron Properties at the Magnetic Pile-up Boundary of Comet P/Halley', *Geophys. Res. Lett.* **16**, 1035.

Mazelle, C. *et al.*, 'The Magnetic Pileup Boundary at Mars: A Comet-like Feature in the Interaction of the Planet Atmosphere with the Solar Wind', this issue.

Mitchell, D. L., Lin, R. P., Rème, H., Crider, D. H., Cloutier, P. A., Connerney, J. E. P., Acuña, M. H. and Ness, N. F.: 2000, 'Oxygen Auger Electrons Observed in Mars' ionosphere', *Geophys. Res. Lett.* **27**, 1871.

Neubauer, F. M. *et al.*: 1986, 'First Results from the Giotto Magnetometer Experiment at Comet Halley', *Nature* **321**, 352.

Paschmann, G., Sckopke, N., Haerendel, G., Papamastorakis, J., Bame, S. J., Asbridge, J.R., Gosling, J. T., Hones, E. W. Jr and Tech, E. R.: 1978, 'ISEE Plasma Observations near the Subsolar Magnetopause', *Space Sci. Rev.* **22**, 717.

Paschmann, G., Baumjohann, W., Sckopke, N., Phan, T. D. and Lühr, H.: 1993, 'Structure of the Dayside Magnetopause for Low Magnetic Shear, *J. Geophys. Res.* **98**, 13 409.

Phan, T. D., Paschmann, G., Baumjohann, W., Sckopke, N. and Lühr, H.: 1994, 'The Magnetosheath Region Adjacent to the Dayside Magnetopause: AMPTE/IRM Observations', *J. Geophys. Res.* **99**, 121.

Phan, T. D. *et al.*: 1996, 'The Subsolar Magnetopause for High Solar Wind Ram Pressure: WIND Observations', *Geophys. Res. Lett.* **23**, 1279.

Phan, T. D. *et al.*: 1997, 'Low-latitude Dusk Flank Magnetosheath, Magnetopause and Boundary Layer for Low Magnetic Shear: Wind Observations', *J. Geophys. Res.* **102**, 19 883.

Sauer, K., Bogdanov, A. and Baumgartel, K.: 1995, 'The Protonopause-an Ion Composition Boundary in the Magnetosheath of Comets, Venus and Mars', *Adv. Space Res.* **16**(4), 153.

Sauer, K. and Dubinin, E.: 2000, 'The Nature of the Martian 'Obstacle Boundary'', *Adv. Space. Res.* **26**, 1633.

Shah, M. B., Elliot, D. S. and Gilbody, H. B.: 1987, 'Pulsed Cross-Beam Study of the Ionisation of Atomic Hydrogen by Electron Impact', *J. Phys. B.* **20**, 3501.

Slavin, J. A. and Holzer, R. E.: 1982, 'The Solar Wind Interaction with Mars Revisited', *J. Geophys. Res.* **87**, 10 285.

Song, P., Russell, C. T., Fitzenreiter, R. J., Gosling, J. T., Thomsen, M. F., Mitchell, D. G., Fuselier, S. A., Parks, G. K., Anderson, R. R., Hubert, D.: 1993, 'Structure and Properties of the Subsolar Magnetopause for Northward Interplanetary Magnetic Field - Multiple-instrument Particle Observations', *J. Geophys. res.* **98**, 11 319.

Sonnerup, B. U. Ö and Cahill Jr., L. J.: 1967, 'Magnetopause Structure and Attitude from Explorer 12 Observations', *J. Geophys. Res.* **72**, 171.

Spreiter, J. R., Summers, A. L. and Alksne, A. Y.: 1966, 'Hydromagnetic Flow around the Magnetosphere', *Planetary Space Sci.* **14**, 223.

Thompson, W. R., Shah, M. B. and Gilbody, H. B.: 1995, 'Single and Double Ionization of Atomic Oxygen by Electron Impact', *J. Phys.* **B28**, 1321.

Trotignon, J. G., Dubinin, E., Grard, R., Barabash, S. and Lundin, R.: 1996, 'Martian Planetopause as Seen by the Plasma Wave System Onboard Phobos 2', *J. Geophys. Res.* **101**, 24 965.

Tsurutani, B. T., Smith, E. J., Anderson, R. R., Ogilvie, K. W., Scudder, J. D., Baker, D. N. and Bame, S. J.: 1982, 'Lion Roars and Nonoscillatory Drift Mirror Waves in the Magnetosheath', *J. Geophys. Res.* **87**, 6060.

Vignes, D., Mazelle, C., Rème, H., Acuña, M. H., Connerney, J. .E. P., Lin, R. P., Mitchell, D. L., Cloutier, P., Crider, D. H. and Ness, N. F.: 2000, 'The Solar Wind Interaction with Mars: Locations and Shapes of the Bow Shock and the Magnetic Pile-up Boundary from the Observations of the MAG/ER Experiment Onboard Mars Global Surveyor', *Geophys. Res. Lett.* **27**, 49.

Zwan, B. J. and Wolf, R. A.: 1976, 'Depletion of Solar Wind Plasma Near a Planetary Boundary', *J. Geophys. Res.* **81**, 1636.